

Light scattering from gap excitations and bound states in SmB_6

P. Nyhus and S. L. Cooper

Department of Physics and Frederick Seitz Materials Research Laboratory, University of Illinois, Urbana-Champaign, Urbana, Illinois 61801

Z. Fisk and J. Sarrao

Department of Physics and National High Magnetic Field Laboratory, Florida State University, Tallahassee, Florida 32306
(Received 5 July 1995)

Gap formation and in-gap bound states are investigated in SmB_6 using Raman scattering. Below 70 K, we observe an abrupt suppression of electronic scattering below $\sim 290 \text{ cm}^{-1}$ that is not consistent with the predicted temperature dependence of a hybridization gap. We also find that gap formation in SmB_6 is associated with the appearance of a sharp $E_g(\Gamma_3^+)$ symmetry 130-cm^{-1} excitation. We discuss several possible interpretations of this excitation, including a $\Gamma_7-\Gamma_8$ crystal-field transition and a transition between bound $4f^5 5d$ configurations.

SmB_6 has been suggested to belong to an interesting group of mixed-valence compounds known as Kondo insulators,¹ which have high-temperature properties typical of Kondo metals, including local moment behavior and strong Kondo scattering of carriers, but have the low-temperature properties of nonmagnetic, small-gap semiconductors [$\Delta \sim 4\text{--}14 \text{ meV}$ in SmB_6 (Refs. 2–4)]. There is still substantial debate concerning the nature of the ground and low-lying excited states in the Kondo insulators. One description of these materials is based on the noninteracting ($U=0$) periodic Anderson model (PAM) at half-filling, which predicts an insulating “hybridization” gap at $T=0$ due to coherent hybridization between the broad $5d\text{--}6s$ conduction band and the localized f states. However, Kondo insulators have also been described by the PAM in the large Kondo coupling regime ($J \rightarrow \infty$), whose ground state is a collection of local singlets, each comprised of a localized spin bound to a conduction electron. Excitations out of this ground state are expected to include spin gap excitations ($\sim \Delta_s$) between singlet and triplet bound-state configurations, and charge gap excitations ($\Delta \geq \Delta_s$) associated with the delocalization of the bound charge.⁵ The importance of charge fluctuations⁶ and the Coulomb interaction⁷ in Kondo insulators has also been stressed. Finally, the ground state of SmB_6 has also been associated with other exotic states, such as a Wigner crystal⁸ and a $4f^6 + 4f^5 \bar{d}$ excitonic state with $A_{1g}(\Gamma_1^+)$ symmetry.⁹

As a powerful tool for studying the energy and symmetry of both dipole-allowed and -forbidden excitations, Raman scattering promises to be useful for elucidating the nature of the ground and low-energy excited states of correlation gap insulators. For example, recent studies of FeSi have demonstrated the efficacy of light scattering for studying energy-gap development in such systems.¹⁰ In this paper, we present a Raman-scattering study of gap formation and in-gap bound states in SmB_6 .

Raman-scattering measurements were performed on the (100) surfaces of single-crystalline SmB_6 prepared from an aluminum flux. The measurements were performed in a vari-

able-temperature He cryostat, using a Spex Triplemate spectrometer equipped with a nitrogen-cooled charge-coupled device array detector. Spectra were obtained with the incident and scattered light polarized in the following configurations in order to identify the symmetries of the excitations studied: $(\mathbf{E}_i, \mathbf{E}_s) = (\mathbf{x}, \mathbf{x})$, $A_{1g} + E_g$; $(\mathbf{E}_i, \mathbf{E}_s) = (\mathbf{x}, \mathbf{y})$, $T_{2g} + T_{1g}$; $(\mathbf{E}_i, \mathbf{E}_s) = (\mathbf{x} + \mathbf{y}, \mathbf{x} + \mathbf{y})$, $A_{1g} + \frac{1}{2}E_g + T_{2g}$; $(\mathbf{E}_i, \mathbf{E}_s) = (\mathbf{x} + \mathbf{y}, \mathbf{x} - \mathbf{y})$, $\frac{3}{4}E_g + T_{1g}$; where \mathbf{E}_i and \mathbf{E}_s are the incident and scattered electric-field polarizations, respectively, \mathbf{x} and \mathbf{y} are the [100] and [010] crystal directions, respectively, and where $A_{1g}(\Gamma_1^+)$, $E_g(\Gamma_3^+)$, and $T_{2g}/T_{1g}(\Gamma_5^+/\Gamma_4^+)$ are the singly, doubly, and triply degenerate irreducible representations of the SmB_6 space group ($O_h^1\text{-}Pm\bar{3}m$), respectively.

Figure 1 shows the Raman-scattering response function, $R''(\omega) = S(\omega)/[1 + n(\omega)]$, of SmB_6 for various temperatures and frequency ranges, where $R''(\omega)$ is obtained from the measured Raman-scattering intensity $S(\omega)$ by dividing out the thermal factor $[1 + n(\omega)] = [1 - \exp(-\hbar\omega/k_B T)]^{-1}$. The room-temperature, high-frequency Raman response of SmB_6 in the inset of Fig. 1 shows the three Raman-active phonon modes allowed by the $O_h^1\text{-}Pm\bar{3}m$ space group, a T_{2g} mode at 730 cm^{-1} , an E_g mode at 1148 cm^{-1} , and an A_{1g} mode at 1280 cm^{-1} , all of which were observed previously by Mörke, Dvorak, and Wachter.¹¹ Additionally, the room-temperature Raman spectrum (inset, Fig. 1) exhibits a broad electronic Raman-scattering background that rises linearly at low frequencies with a broad peak near 1200 cm^{-1} , and a defect-induced phonon mode with T_{2g} symmetry near 163 cm^{-1} whose intensity decreases roughly sixfold below 300 K. This “defect-induced” mode in SmB_6 was recently attributed to an “extra” vibrational mode induced by nonadiabatic coupling of the lattice to valence fluctuations.¹² A complete examination of the 163-cm^{-1} mode in the context of this description is given by Lemmens *et al.*¹³

The low-temperature, low-frequency Raman response of SmB_6 is illustrated in the main part of Fig. 1. One of the most dramatic features of the low-temperature Raman response in SmB_6 is an abrupt suppression of electronic scat-

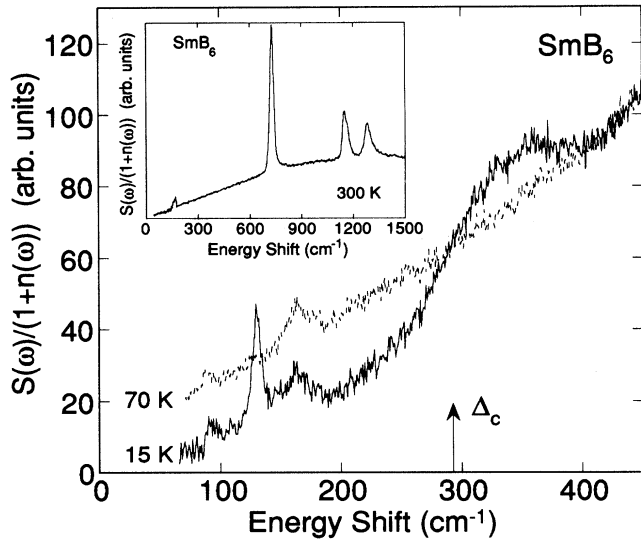


FIG. 1. Comparison of the 70- and 15-K $A_{1g} + E_g + T_{2g}$ symmetry Raman-scattering response functions, $R''(\omega) = S(\omega)/[1 + n(\omega)]$, of SmB_6 , where $S(\omega)$ is the measured Raman-scattering intensity and $[1 + n(\omega)] = [1 - \exp(-\hbar\omega/k_B T)]^{-1}$ is the thermal factor. A suppression of electronic Raman scattering below $\Delta_c \sim 290 \text{ cm}^{-1}$, and a redistribution of electronic scattering strength to the energy range $300 \leq \omega \leq 400 \text{ cm}^{-1}$, is apparent in SmB_6 due to the development of an energy gap. Also evident in the 15-K spectrum is a sharp E_g symmetry excitation that develops abruptly near 130 cm^{-1} for $T < 45 \text{ K}$. Inset: Room-temperature, high-frequency Raman-scattering response function $R''(\omega)$ for SmB_6 , exhibiting optical phonons at 780 cm^{-1} (T_{2g}), 1148 cm^{-1} (E_g), and 1280 cm^{-1} (A_{1g}), and a defect-induced phonon mode at 163 cm^{-1} .

tering below $\sim 290 \text{ cm}^{-1}$, and a corresponding enhancement of electronic scattering intensity between 300 and 400 cm^{-1} , reflecting the development of an energy gap in SmB_6 for $T < 70 \text{ K}$. A similar redistribution of electronic Raman scattering due to the development of a gap ($\sim 780 \text{ cm}^{-1}$) was also observed in the correlation gap insulator FeSi .¹⁰ Previous estimates of the gap in SmB_6 were obtained from resistivity ($\Delta \sim 4 \text{ meV}$),² optical ($\Delta \sim 4\text{--}14 \text{ meV}$),^{3,4} and point-contact spectroscopy¹⁴ ($\Delta \sim 5 \text{ meV}$) measurements. The smallest of these gap values correspond roughly to the frequency below which the low-temperature electronic Raman-scattering intensity goes to zero (see Fig. 1). However, our Raman-scattering results show that energy-gap formation in SmB_6 involves a suppression of electronic spectral weight over a substantially larger frequency range, $\Delta_c \sim 290 \text{ cm}^{-1}$, than the estimated transport gap, $\Delta_{\text{tr}} \sim 30 \text{ cm}^{-1}$. Notably, Δ_c is comparable to the maximum energy for which the optical conductivity in SmB_6 is suppressed by gap formation,⁴ and is close to the onset energy of an optical absorption band that has been identified as the (direct) d - f optical gap.³

Figure 1 also shows that the suppression of spectral weight due to gap formation in SmB_6 is incomplete below Δ_c , revealing a broad spectrum of in-gap states with a roughly quadratic frequency dependence, $S(\omega) \sim \omega^2$, at low temperatures. A careful polarization study of the gap shows

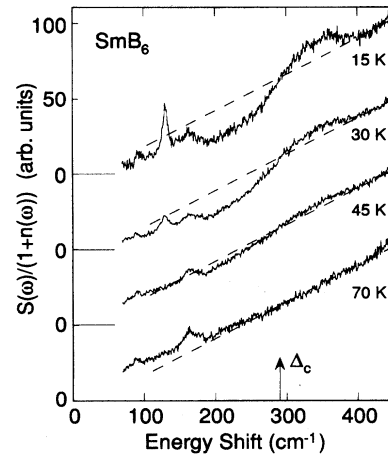


FIG. 2. The $A_{1g} + E_g + T_{2g}$ symmetry Raman-scattering response function, $R''(\omega) = S(\omega)/[1 + n(\omega)]$, of SmB_6 at various temperatures, illustrating (i) the suppression of electronic scattering below $\Delta_c = 290 \text{ cm}^{-1}$ for $T < 70 \text{ K}$ and (ii) the development of the E_g symmetry mode near 130 cm^{-1} for $T < 45 \text{ K}$.

no evidence for anisotropy in either Δ_c or the frequency dependence of in-gap states, although the electronic Raman-scattering intensity is strongest in A_{1g} and E_g geometries. Additionally, Fig. 2 illustrates that the energy below which electronic scattering is suppressed, Δ_c , is essentially independent of temperature once the gap begins to form, and thus represents a fixed energy scale across which spectral weight is systematically redistributed by the developing gap.

The 15-K Raman spectrum (Fig. 1) also reveals that the opening of an energy gap in SmB_6 is accompanied by the development of a sharp $E_g(\Gamma_3^+)$ symmetry excitation at 130 cm^{-1} (16 meV), an energy quite close to the optical absorption edge observed in SmB_6 [$\sim 120 \text{ cm}^{-1}$ (Ref. 4)]. The intensity of this excitation is roughly a factor of 5 smaller than the intensity of the weakest optical phonon. Figure 2 shows that the 130-cm^{-1} $E_g(\Gamma_3^+)$ Raman mode disappears abruptly for $T > 30 \text{ K}$, suggesting that this excitation is either screened or strongly damped by thermally excited carriers in the d band. Neutron-scattering studies^{15,16} of SmB_6 have also observed this mode at lower energy, $E = 13 \text{ meV}$ ($\sim 104 \text{ cm}^{-1}$), and at higher momentum transfer, $|\mathbf{q}| = 1.3 \text{ \AA}^{-1}$,¹⁶ although a symmetry determination of the excitation could not be made with these measurements.

The evolution of a sharp excitation within the optical gap in SmB_6 is suggestive of an impurity level. However, the 130-cm^{-1} excitation is not consistent with a Wannier-Mott-type exciton associated with localized in-gap states, since optical estimates³ of the mass renormalization, $m^*/m_e \sim 1.5$, and the effective dielectric response, $\epsilon \sim 500$, in SmB_6 imply a binding energy, $E_B = (13.6 \text{ eV})(m^*/\epsilon^2 m_e) \sim 1 \text{ K}$, that is too small, and an exciton radius, $r_{\text{ex}} = (0.53 \text{ \AA})(\epsilon m_e/m^*) \sim 170 \text{ \AA}$, that is much larger than the $\sim 2\text{-\AA}$ radial extent of this excitation estimated from neutron-scattering measurements.¹⁶ One possibility that we cannot rule out is that the 130-cm^{-1} excitation is a Frenkel-type exciton, such as an f - d exciton involving an electron released from the $4f$ shell that bound to the $4f$ hole left behind.

Two particularly notable interpretations are consistent with the symmetry, energy, and temperature dependence of the 130-cm^{-1} E_g excitation. The first is a crystal-field transition between Γ_7 doublet and Γ_8 quartet levels of the $4f^5$ ${}^6H_{5/2}$ manifold (Sm^{3+}). The E_g symmetry of the 130-cm^{-1} Raman excitation in SmB_6 is indeed consistent with a $\Gamma_7 \rightarrow \Gamma_8$ transition, $\Gamma_7 \otimes \Gamma_8 = E_g \oplus T_{1g} \oplus T_{2g}$ ($\Gamma_3^+ \oplus \Gamma_4^+ \oplus \Gamma_5^+$), and the 130-cm^{-1} energy is close to the Sm^{3+} (${}^6H_{5/2}$) Γ_7 - Γ_8 energy splitting estimated from crystal-field parameters, $\Delta_{\text{CF}} \sim 103\text{ cm}^{-1}$.¹⁷ Furthermore, while crystal-field excitations generally exhibit a significant temperature dependence only for $T \geq \Delta_{\text{CF}}$ ($\sim 180\text{ K}$ in SmB_6), the abrupt temperature dependence of the E_g mode in SmB_6 (see Fig. 2) could result from the rapid development of the gap below 70 K , which should substantially reduce f - d hybridization for $\omega < \Delta_c$. It should also be noted that the observation of pure intraionic $4f^5$ transitions is not precluded in configurationally mixed materials such as SmB_6 when the energy transferred to the system is larger than the hybridization energy. Under these circumstances, one expects to probe a static mixture of $4f^6$ and $4f^5$ configurations.¹⁸ Indeed, neutron-scattering studies of SmB_6 report both the ($4f^5$) $J = \frac{5}{2} \rightarrow J = \frac{7}{2}$ ($\sim 1000\text{ cm}^{-1}$) and ($4f^6$) $J = 0 \rightarrow J = 1$ ($\sim 300\text{ cm}^{-1}$) intermultiplet transitions at low temperatures.¹⁶ Perhaps the strongest argument against the crystal-field interpretation is that the \mathbf{q} dependence of the 130-cm^{-1} excitation does not follow the single-ion $4f$ form factor, but rather a form factor that betrays some mixture of f - and d -orbital character.¹⁶

A second noteworthy scenario is that the 130-cm^{-1} $E_g(\Gamma_3^+)$ mode involves an interconfigurational (valence-conserving) transition from the ground singlet state to a bound excited state. The exact nature of such a transition depends upon assumptions about the ground state. One possibility, which presumes that the ground state is partly comprised of a $4f^5$ (${}^6H_{5/2}$) state bound to a spin- $\frac{1}{2}$ $5d(e_g)$ conduction electron in a parallel spin configuration, $4f^5 5d^1$ (7H_2),¹⁹ is that the 130-cm^{-1} mode involves a spin-flip transition to a $4f^5 5d^1$ state with antiparallel spin alignment (5H_3). However, neutron-scattering measurements find that the 130-cm^{-1} mode has a highly anisotropic \mathbf{q} dependence,¹⁶ suggesting that this excitation has a d -orbital contribution that is distributed in an extended wave function on the nearest-neighbor Sm sites. An example of such a bound state has been proposed by Kikoin and Mishchenko,⁹ who argue that intermediate-valent SmB_6 has singlet (A_{1g}) ground (Ψ_g) and excited (Ψ_e) states described by $\Psi_{g,e} = |4f^6\rangle \pm |4f^5 \bar{d}_{\Gamma_7^-}\rangle$, where the second term represents a small-radius excitonic state comprised of a $4f^5$ hole on one Sm site bound to an electron shared in a Γ_7^- -symmetry linear combination of $5d$ orbitals on the six nearest-neighbor Sm sites, $\bar{d}_{\Gamma_7^-}$. This model predicts a monopolar (A_{1g}) transition between bonding (Ψ_g) and antibonding (Ψ_e) configurations, involving a change in both spin and orbital degrees of freedom.

Significantly, the E_g symmetry of the 130-cm^{-1} excitation rules out a monopolar bound-state transition, but is consistent with a quadrupolar transition from a bound singlet state ($A_{1g}; J=0$) to an E_g symmetry $4f^5 \bar{d}$ bound state (E_g

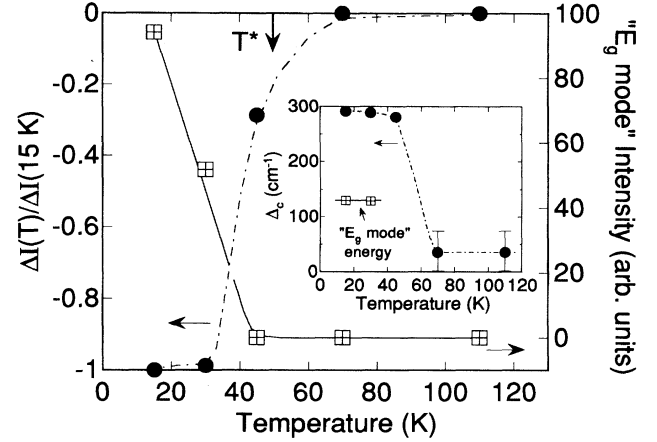


FIG. 3. Filled circles: Temperature dependence of the fractional change in integrated electronic spectral weight below $\Delta_c \sim 290\text{ cm}^{-1}$, $\Delta I(T)/\Delta I(T=15\text{ K})$, where $\Delta I(T) = I(T) - I(340\text{ K})$, and $I(T)$ is the integrated electronic spectral weight associated with the Raman response function $R''(\omega)$ below $\omega = \Delta_c$. Open squares: Temperature dependence of the integrated E_g mode intensity. Inset: Plot of Δ_c as a function of temperature (filled circles), where Δ_c is the energy below which electronic Raman-scattering intensity in $R''(\omega)$ is suppressed with decreasing temperature compared to the 70-K spectrum (see Fig. 2). For comparison, the E_g mode energy is also plotted as a function of temperature (open squares). The error bars reflect uncertainty in determining Δ_c below 75 cm^{-1} .

$\in \Gamma_7^- \otimes \Gamma_8^-; J=2$). Several possible orbital configurations of the extended d state are compatible with such a bound state. For example, an E_g symmetry $4f^5 \bar{d}$ bound state can be constructed from the Γ_7^- ($4f^5$) state on a Sm site bound to an electron in a Γ_8^- symmetry combination of $5d$ states on the six nearest-neighbor Sm sites. As the spin contribution to the spin- $\frac{1}{2}$ d -electron wave function transforms like Γ_6^+ , the possible orbital configurations of a Γ_8^- symmetry extended state have e_u , t_{1u} , or t_{2u} symmetry [$\Gamma_8^- \in \Gamma_6^+ \otimes (e_u, t_{1u}, t_{2u})$]. Alternatively, an E_g symmetry $4f^5 \bar{d}$ state can involve the Γ_8^- part of the $4f^5$ state bound to a Γ_7^- symmetry combination of $5d$ states. A Γ_7^- symmetry extended state is consistent with either a_{2u} or t_{2u} symmetry orbital configurations on the six nearest neighbors. The Raman-scattering process associated with this bound-state excitation can occur via a two-step $4f^6 \leftrightarrow 4f^5 5d$ interconfigurational transition that should be resonant with the $4f^6 \rightarrow 4f^5 5d(t_{2g})$ optical transition.

The relationship between gap formation and the development of the 130-cm^{-1} is summarized in Fig. 3. The filled circles in the main part of Fig. 3 illustrate, as a function of temperature, the fractional change in the integrated electronic scattering intensity below $\Delta_c \sim 290\text{ cm}^{-1}$, $\Delta I(T)/\Delta I(T=15\text{ K})$, where $\Delta I(T) = I(T) - I(110\text{ K})$, and $I(T) = \int_0^{\Delta_c} R''_e(\omega; T) d\omega$ is the integrated spectral weight associated with the electronic contribution to the Raman-scattering response function $R''_e(\omega)$ below $\Delta_c \sim 290\text{ cm}^{-1}$ at a given temperature T . The open squares compare the integrated intensity of the 130-cm^{-1} E_g excitation as a function of temperature, showing that it develops rapidly as low-frequency electronic scattering strength is suppressed by gap formation.

Figures 2 and 3 illustrate several key characteristics of gap development in SmB_6 : an abrupt suppression of electronic scattering for (a) temperatures below $T^* \sim 50$ K [roughly the temperature at which the peak in the magnetic susceptibility is observed in SmB_6 (Ref. 19)], and (b) energies less than a temperature-independent energy scale, $\Delta_c \sim 8k_B T^*$. Neither of these characteristics is consistent with conventional hybridization gap models in which a temperature-dependent (indirect) gap forms gradually at low temperatures.²⁰ The primary issues raised by these results concern the proper interpretation of Δ_c and the nature of the in-gap states observed in SmB_6 . Cooley *et al.* suggest that the in-gap states observed in SmB_6 are akin to the many-body states that develop below a Mott-Hubbard transition.² Indeed, the doping-induced collapse of the optical gap observed in certain charge-transfer and Mott-Hubbard insulators shares certain similarities with the temperature-dependence of the gap in SmB_6 , including a rapid redistribution of spectral weight across an “isobestic” fixed point and a rapid introduction of states within the gap.²¹ Alternatively, Bucher *et al.* find that the suppression of low-frequency optical conductivity below T^* in the Kondo insulator $\text{Ce}_3\text{Bi}_4\text{Pt}_3$ correlates with the quenching of the $4f$ moment,²² implying that gap formation in this material is more appropriately associated with the formation of local singlets. A similar description provides a consistent interpretation of our SmB_6 results, namely, that the suppression of electronic scattering below T^* (filled circles in Fig. 3) re-

fects the systematic binding of itinerant d electrons into local singlets, while the 130-cm^{-1} excitation below T^* (open squares in Fig. 3) is a “spin-flip”-type excitation between different bound $4f5d$ configurations. In this picture, the temperature independence of the gap, $\Delta_c \sim 290\text{ cm}^{-1}$, in SmB_6 (inset, Fig. 3) is attributable to the temperature independence of the Kondo temperature, $\Delta_c \sim k_B T_K$. It is interesting to note that the results described here for SmB_6 are remarkably similar to those observed in the Kondo insulator $\text{Ce}_3\text{Bi}_4\text{Pt}_3$, which exhibits a temperature-independent charge gap of $\Delta_c \sim 300\text{ cm}^{-1}$,²² and a spin gap of $\Delta_s \sim 160\text{ cm}^{-1}$.²³

In summary, we find that gap development below $T^* \sim 50$ K in SmB_6 is characterized by an abrupt suppression of electronic Raman-scattering intensity below a temperature-independent energy scale $\Delta_c \sim 290\text{ cm}^{-1}$, by the presence of a broad spectrum of localized in-gap states with frequency dependence $S(\omega) \sim \omega^2$, and by the appearance of a sharp E_g symmetry excitation near 130 cm^{-1} . The latter is associated with a bound-state excitation formed between a $4f^5$ state and a d electron which may occupy an extended state on nearest-neighbor Sm sites.

This work was supported by Grant No. NSF DMR 91-20000 through the STCS (P.N. and S.L.C.) and by the NHMFL through Grant No. NSF DMR 90-16241 (Z.F.). We acknowledge use of the MRL Laser Lab Facility.

¹G. Aeppli and Z. Fisk, *Comments Condens. Matter Phys.* **16**, 155 (1992).

²J. C. Cooley, M. C. Aronson, Z. Fisk, and P. C. Canfield, *Phys. Rev. Lett.* **74**, 1629 (1995).

³G. Travaglini and P. Wachter, *Phys. Rev. B* **29**, 893 (1984).

⁴T. Nanba, H. Ohta, M. Motokawa, S. Kimura, S. Kunii, and T. Kasuya, *Physica B* **186-188**, 440 (1993).

⁵K. Ueda, M. Sigrist, H. Tsunetsugu, and T. Nishino, *Physica B* **194-196**, 255 (1994).

⁶C. M. Varma, *Phys. Rev. B* **50**, 9952 (1994).

⁷T. Kasuya, *Europhys. Lett.* **26**, 277 (1994).

⁸T. Kasuya, K. Takegahara, T. Fujita, T. Tanaka, and E. Bannai, *J. Phys. (Paris) Colloq.* **40**, C5-308 (1979).

⁹K. A. Kikoin and A. S. Mishchenko, *J. Phys. Condens. Matter* **2**, 6491 (1990).

¹⁰P. Nyhus, S. L. Cooper, and Z. Fisk, *Phys. Rev. B* **51**, 15 626 (1995).

¹¹I. Mörke, V. Dvorak, and P. Wachter, *Solid State Commun.* **40**, 331 (1981).

¹²K. A. Kikoin and A. S. Mishchenko, *Zh. Éksp. Teor. Fiz.* **104**, 3810 (1993) [*JETP* **77**, 828 (1993)].

¹³P. Lemmens, A. Hoffman, A. S. Mischenko, M. Yu. Talantov, and

G. Güntherodt, *Physica B* **206&207**, 371 (1995).

¹⁴I. Frankowski and P. Wachter, *Solid State Commun.* **41**, 577 (1982).

¹⁵E. Holland-Moritz and M. Kasaya, *Physica B* **136**, 424 (1986).

¹⁶P. A. Alekseev, *Physica B* **186-188**, 365 (1993).

¹⁷D. B. McWhan, S. M. Shapiro, J. Eckert, M. A. Mook, and R. J. Birgeneau, *Phys. Rev. B* **18**, 3623 (1978).

¹⁸See, for example, P. Wachter, in *Handbook on the Physics and Chemistry of Rare Earths*, edited by K. A. Gschneider, Jr. and L. Eyring (North-Holland, Amsterdam, 1993), Vol. 19, p. 177.

¹⁹J. C. Nickerson, R. W. White, K. N. Lee, R. Bacimann, T. H. Geballe, and G. W. Hull, Jr., *Phys. Rev. B* **3**, 2030 (1971).

²⁰C. Sanchez-Castro, K. S. Bedell, and B. R. Cooper, *Phys. Rev. B* **47**, 6879 (1993).

²¹S. Uchida, T. Ido, H. Takagi, T. Arima, Y. Tokura, and S. Tajima, *Phys. Rev. B* **43**, 7942 (1991); E. Dagotto, *Rev. Mod. Phys.* **66**, 763 (1994).

²²B. Bucher, Z. Schlesinger, P. C. Canfield, and Z. Fisk, *Phys. Rev. Lett.* **72**, 522 (1994).

²³A. Severing, J. D. Thompson, P. C. Canfield, Z. Fisk, and P. Riseborough, *Phys. Rev. B* **44**, 6832 (1991).